Available online at www.sciencedirect.com
ScienceDirect
Journal of Power Sources 177 (2008) 546–552
JOURNAL OF POWER SOURCES
www.elsevier.com/locate/jpowsour

CoO-loaded graphitable carbon hollow spheres as anode materials for lithium-ion battery

Feng Li, Qing-Qing Zou, Yong-Yao Xia *

Department of Chemistry and Shanghai Key Laboratory of Molecular Catalysis and Innovative Materials, Fudan University, Shanghai 200433, China

Received 29 August 2007; accepted 26 October 2007
Available online 4 December 2007

Abstract

A new type of CoO nanoparticles encapsulated by graphitable hollow carbon sphere (GHCS) composite material was synthesized. The core–shell structure CoO/GHCS composite shows the improved cyclability as an anodic material in Li-ion battery. The core–shell composite containing 50 wt% CoO exhibits a reversible capacity of 584 mAh g^{-1} at a constant current density of 100 mA g^{-1} between 0 and 3.0 V (vs. Li^+/Li), and remains a capacity retention of 95% after 50th cycle. The improvement could be attributed to that the GHCS with a good electronic conductivity and high surface severs as dispersing medium to prevent CoO nanoparticles from aggregating, and provide the enough space to buffer the volume change during the Li-ion insertion and extraction reactions in CoO nanoparticles.

Keywords: Graphitable hollow carbon sphere; CoO; Lithium-ion battery

1. Introduction

Lithium-ion battery has been considered as a promising power source for the modern electronic applications due to its highest energy density among commercial rechargeable batteries. However, the theoretical capacity of the graphite is limited to be 372 mAh g^{-1} due to the formation of LiC_6 [1–3]. Poizot et al. [4] proposed a class of new anode materials, nano-sized transition-metal oxide (MO, where M is Co, Ni, Cu or Fe), which can obtain high reversible specific capacity when used as the anodic materials of lithium-ion batteries [5–8]. Among them, cobalt oxide was demonstrated the best electrochemical properties as lithium storage materials in Li-ion battery. Different from the carbonaceous compounds or lithium-alloying processes, the reversible electrochemical reaction mechanism of the charge/discharge process for CoO was mentioned to be the formation and decomposition of Li_2O, accompanying the reduction and oxidation of metal nanoparticles [4,9]. However, similar to most other nanomaterials, the cycling performances of CoO are extremely sensitive to their degree of aggregation. Severe particle aggregation leads to significant capacity fading due to deteriorated electric contact between particles, therefore a high capacity can only remain with the well dispersion of CoO particles on some substrate materials (for example carbon).

As the substrate materials, various carbon materials have been used severing as dispersing and electronic medium. Yang et al. [8] reported a composite material of Co_3O_4 and porous hard carbon spherules. It exhibited better cycling performance than pure Co_3O_4, and reversible capacity can reach 420 mAh g^{-1}. Huang et al. [10] synthesized a series of graphite–metal oxide (G-MO, M = Cu, Fe, Ni, Pd etc.) composites, which were able to improve the cyclability and rate capability. Hu et al. [11,12] reported Cr_2O_3 and Cr_2O_3/carbon composite as the anode material for Li-ion batteries. Bare Cr_2O_3 electrodes showed poor cyclic performance due to large volume change, while Cr_2O_3/C composite showed good capacity retention and improved first cycle coulombic efficiency, which could benefit from maintaining good electronic contact of active particles during cycling. In order to obtain high electrochemical performance, carbon material should possess the properties of both the high electronic conductivity and high surface area. The high surface can provide active sites enough for the nanoparticles to be pinned on or embedded on the carbon surface. Meanwhile the high electronic conductivity can reduce the electrode polarization to improve

* Corresponding author. Fax: +86 21 55664177.
E-mail address: yyxia@fudan.edu.cn (Y.-Y. Xia).

0378-7753/$ – see front matter © 2007 Elsevier B.V. All rights reserved.
doi:10.1016/j.jpowsour.2007.10.097

both the cycling stability and rate performance. Wang et al. [13] reported a type of SnO_2/crystalline hollow carbon spheres in which the SnO_2 nanoparticles were loaded on both the external and inside surface of the carbon. The SnO_2/carbon composite material exhibited good electrochemical performance. Here, we prepared a type of graphitable hollow carbon spheres (named as GHCS) with high surface area, which was used to load cobalt oxide particles by wet-penetration method. The graphitable hollow carbon spheres serve as a supporting material preventing from CoO particle agglomeration, as well as behave a host for Li-storage. The effect of CoO mass load on the specific capacity, cycling stability and rate capability was evaluated as negative electrode for Li-ion batteries.

2. Experimental

The silica spheres with a uniform diameter of 500 nm were obtained by the Stober method [14]. Two hundred and twenty milliliters of NH_4OH (25%) was added to a mixture of 145 ml of H_2O and 560 ml of ethanol to form a homogeneous solution. Then, a mixed solution of 56 ml of TEOS (tetraethoxysilane) and 50 ml of ethanol was poured in this solution and left overnight at room temperature under stirring. Finally, the monodisperse silica spheres were collected after filtration and washing with distilled water. The graphitable hollow carbon spheres were prepared by the following process: The as-prepared silica spheres were transferred into a quartz tube to make a fluid-bed layer for reaction where a benzene vapor was carried by nitrogen gas through the reaction tube at a flow rate of 50 ml min^{-1}. The reaction temperature was maintained at 950 °C for 5 h. After being cooled in pure flowing nitrogen, the silica spheres coated with carbon were removed by dilute 5% HF solution, and GHCS were obtained after washing with distilled water and drying at 100 °C.

CoO/GHCS composite material was prepared by the following route: 1.0 g carbon spheres were dispersed into 20 ml ethanol solution containing definite amount of $Co(NO_3)_2{\cdot}6H_2O$ in a conical flask. For example, if the target product with CoO mass load of 10 wt%, 0.43 g $Co(NO_3)_2{\cdot}6H_2O$ was added. After completely dissolved, the ethanol solution was vaporized slowly at 70 °C under stirring, and then the CoO/GHCS composite material was obtained after heating the mixture in a tube furnace at 400 °C for 2 h under nitrogen flowing. CoO/GHCS composite materials with different CoO contents, varying from 10, 25, 50 to75 wt% were prepared.

The crystallographic information, grain size and surface morphologies of the as-prepared samples were analyzed by X-ray powder diffraction (XRD, Bucker D8) with Cu Kα radiation from 10° to 90°, Scanning electronic microscope (SEM, Philip XL30) and transmission electron microscopy (TEM, Jeol JEM-2010), respectively. The surface area was determined from N_2 adsorption/desorption isotherms, which were obtained by Micromeritics Tristar.

The negative electrodes were prepared by mixing 90 wt% GHCS/CoO composite material powders, 5 wt% acetylene black, and 5 wt% polyvinylidene fluoride (PVDF) dissolved in *N*-methylpyrrolidinone (NMP). The slurries of the mixture were coated on Cu foil. After coating, the electrodes were dried at 80 °C for 10 min to remove the solvent before pressing. The electrodes were cut into sheets 1 cm^2 in area, vacuum-dried at 100 °C for 24 h, and weighed. The typical mass load of the active material is about 3 mg cm^{-2}. The battery performance was characterized in CR2032-type coin cell. Metallic lithium was used as the negative electrode. The electrolyte solution was 1 M $LiPF_6$/ethlylene carbonate (EC)/dimethyl carbonate (DMC)/ethyl methyl carbonate (EMC) (1:1:1 by volume). The cells were cycled at a constant current density of 100 mA g^{-1} between 0 and 3.0 V. Lithium insertion into the CoO/GHCS electrode was referred to as discharge and extraction as charge. The cell capacity was determined by only the active material (CoO/GHCS). Cyclic voltammograms (CV) were characterized using a three-electrode cell, the metallic lithium was used as a counter and reference electrodes, and it was performed using a Solarton Instrument Model 1287 electrochemical interface controlled by a computer.

3. Result and discussion

GHCS was synthesized by chemical vapor deposition (CVD) of benzene with templates of silica spheres at 950 °C. Fig. 1A gives the SEM image of uniform silica spheres, and Fig. 1B shows the SEM image of silica spheres coated with carbon layer after chemical vapor deposition treatment. From the image, the surface of carbon-loaded silica spheres is rougher than that of silica spheres. Fig. 1C and D shows the SEM and TEM images of GHCS, respectively. It is clearly observed that the integrally spherical morphology is maintained after removing silica core by dilute HF solution, suggesting that the graphitable hollow carbon spheres have high mechanical intensity. Moreover, it can be considered that carbon shell is porous structure to allow the HF solution infiltrating spherical shell completely to remove the silica templates. In our route of synthesis, it was found that the thickness, roughness and mechanical intensity of hollow carbon spheres are determined by the CVD condition, especially the deposition temperature and time. Under the constant saturated vapor pressure of benzene, the stability and the thickness of hollow carbon spheres will be enhanced with the increase of deposition temperature and time.

Fig. 2A and B shows the TEM images of 25 wt% CoO/GHCS composite. From the image, most of CoO nanoparticles adhere to the inner surface, rather than the external surface of GHCS. During the synthetic process, the GHCS were firstly dispersed into the ethanol solution containing $Co(NO_3)_2$, and the ethanol solution can easily penetrate into carbon spherical shell throughout the crack and pore resulting from the discontinuous graphite sheets. With the continuous volatilization of ethanol, the interior solution of GHCS evaporated more slowly than outside solution, which made the outside $Co(NO_3)_2$ with higher concentration diffuse to inner of GHCS, and the inside $Co(NO_3)_2$ was accumulated continuously until the ethanol solution was volatilized completely. After calcinations of mixture, the CoO nanoparticles encapsulated by graphitable hollow carbon spheres were obtained. Fig. 2C and D compares the TEM images of the surface of GHCS and 25 wt% CoO-loaded GHCS, it is noticed that hollow carbon spheres consisted with the closely packed graphite

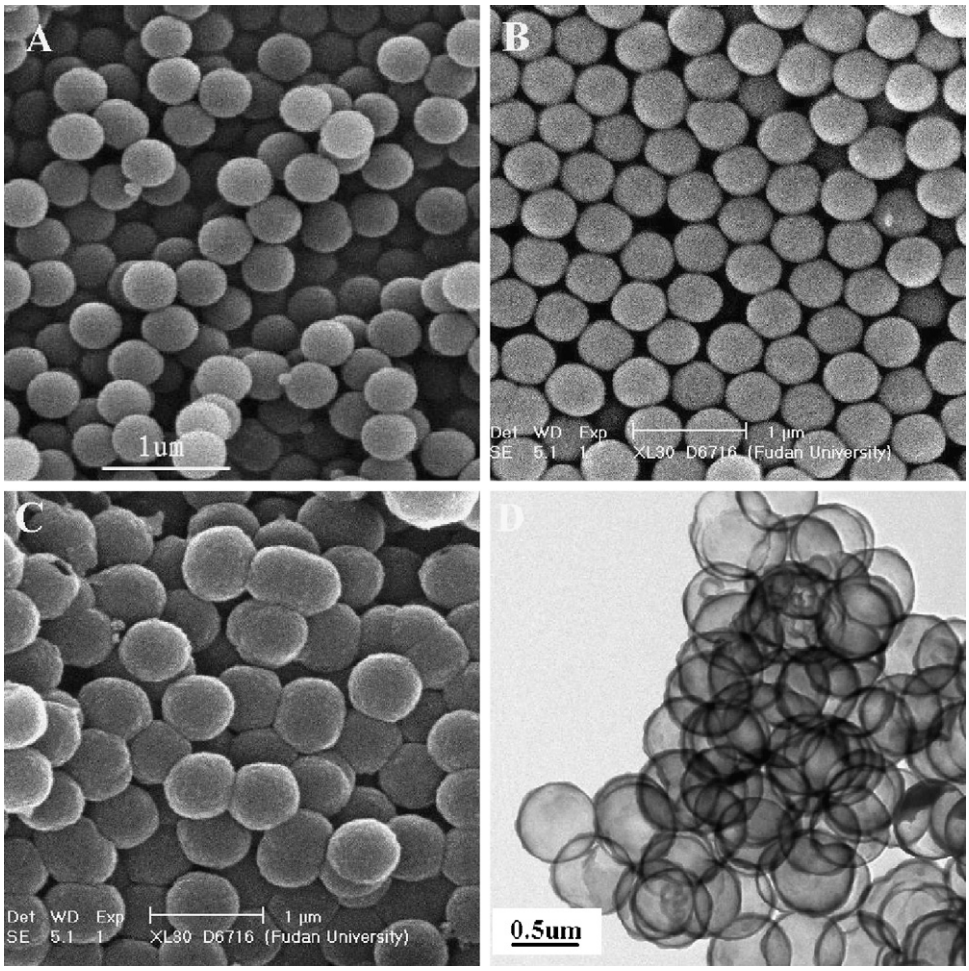

Fig. 1. SEM images of (A) monodisperse silica spheres (B) silica spheres coated with graphitable carbon (C) graphitable hollow carbon spheres. (D) TEM image of graphitable hollow carbon spheres.

sheet aligned approximately parallel to the surface of the carbon shell with thickness ca. 20–30 nm. After wet-penetration by $Co(NO_3)_2$, CoO nanoparticles were accumulated in the inner space of GHCS, and some residue of CoO were remain in the crack and pore between discontinuous graphite sheets.

The XRD patterns of GHCS, 25% CoO-loaded GHCS are shown in Fig. 3. The character diffusion peak at ~25° (0 0 2) and ~44° (1 0 0) demonstrates the presence of graphitic carbon, and the main diffusion peaks at scattering angels (2θ) of 36.6°, 42.6° and 61.8° are assigned to scattering from the 1 1 1, 2 0 0 and 2 2 0 lattice planes, which confirms CoO particles loading on the carbon substrate. The curve of CoO/GHCS shows feebler and broader diffusion peaks, which suggest CoO particles have poorer crystallinity and smaller particle size. The GHCS exhibits a Brunauer–Emmett–Teller (BET) surface area of 65.6 $cm^2\ g^{-1}$ and a total pore volume of 0.36 $cm^3\ g^{-1}$ by the N_2 adsorption–desorption isotherms.

To understand the electrochemical process, the cyclic voltammograms (CV) profiles of the 25 wt% CoO/GHCS composite electrode from the first to the third cycles are recorded in Fig. 4. In the first cycle, there are two obvious reduction peaks. The peak at around 0.1 V corresponds to the insertion of Li into GHCS, and the peak at around 0.6 V is assigned to the reaction of Li-ion inserting GHCS and the formation of Li_2O and Co from the reduction of CoO. It is noticed that the reduction peak at ca. 0.6 V shifts to a higher potential, and become two peaks (one peak at ca. 0.8 V and the other at ca. 1.25 V) in subsequent cycles. The 1.25 V peak is attributed to the reduction reaction of Li with CoO, and the shift of reduction peak might be related to the pulverization of the CoO particles [8]. During the first discharge process, the CoO particles are pulverized during Li-insertion and their surface energy is decreased due to interaction with the produced Li_2O. Hence the potential of Li-insertion become higher in subsequent cycles. Around 0.8 V, the addition of Li-ion inserting GHCS reaction results in the 0.8 V reduction peak higher than the 1.25 V peak. In the oxidation segment of CV profiles, there are three obvious oxidation peaks (0.4, 1.0 and 2.2 V, respectively). Both the strong peak at around 0.4 V and the weak peak at around 1.0 V correspond to the extraction of Li-ion from GHCS, and the oxidation peak at around 2.2 V is attributed to the regeneration of CoO. The reduction peak at 0.6 V in the first cycle, but disappears in the subsequent cycles, is the main contribution of irreversible capacity in the first cycle. The irreversible capacity mainly arises from the formation of SEI layer and the inactivation of some inserted Li-ion.

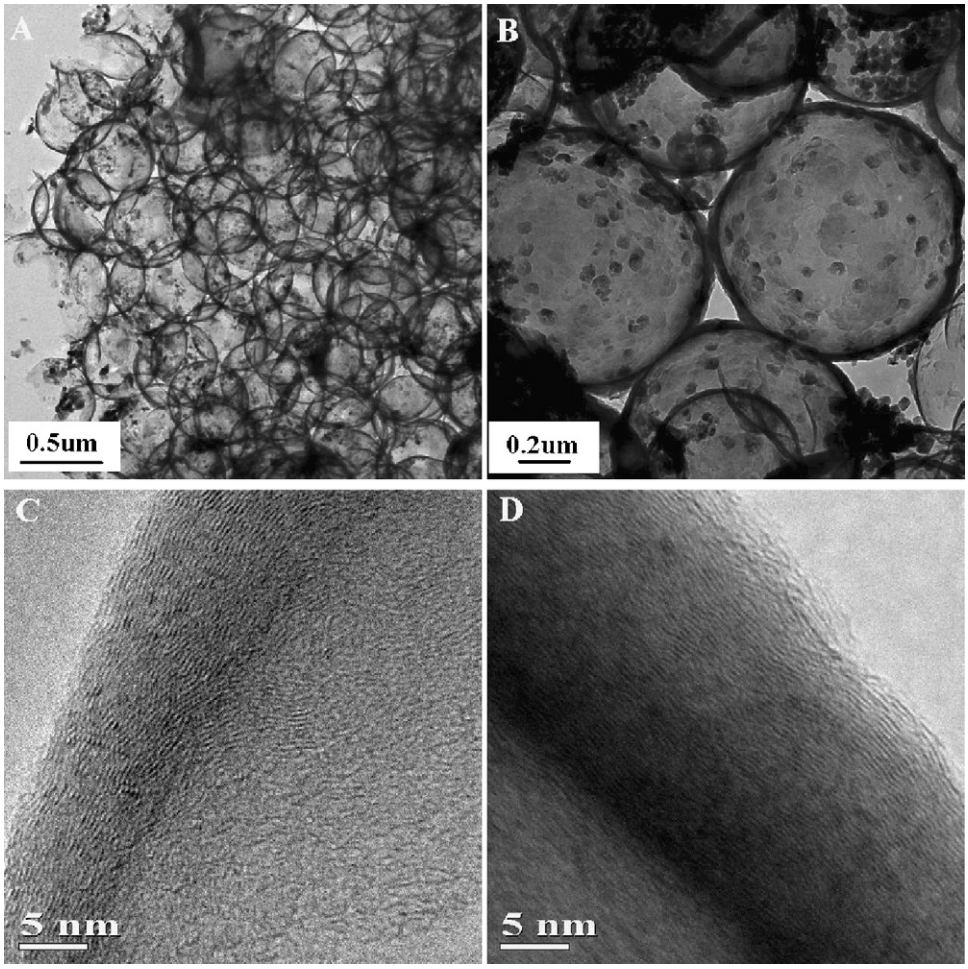

Fig. 2. TEM image of 25 wt% CoO/GHCS composite material (A) low and (B) high-magnification. (C) HRTEM image of GHCS and (D) HRTEM image of 25 wt% CoO/GHCS.

In order to compare the effect of the different mass load of CoO on its electrochemical performance, the CoO/GHCS composite materials with different CoO contents are prepared. The mass load of CoO is 10, 25, 50, 75 wt%, respectively. Fig. 5 gives the typical charge/discharge curves of GHCS with different CoO mass loads (25, 75 wt%) between 0 and 3.0 V (vs. Li^+/Li) at a galvanostatic charge/discharge current of 100 mA g^{-1}. The data was obtained at 1st, 2nd and 50th cycles. For a comparison, the charge/discharge curve of GHCS is also given in Fig. 5A. GHCS exhibits a discharge capacity of 429 mAh g^{-1} and charge

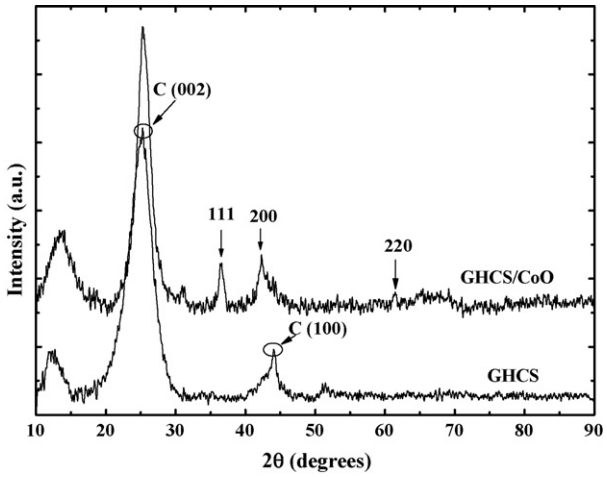

Fig. 3. The XRD patterns of GHCS, 25 wt% CoO/GHCS.

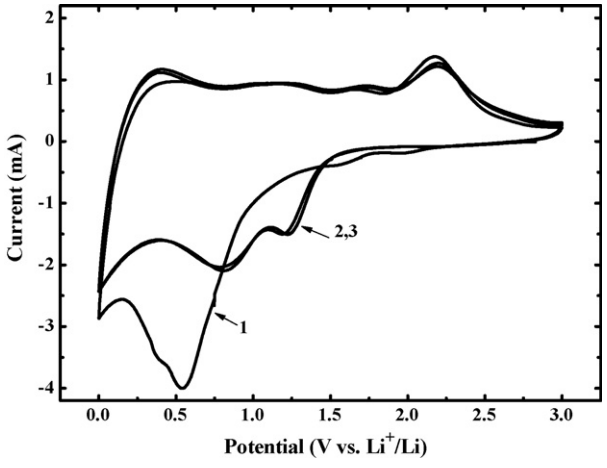

Fig. 4. Cyclic votammograms profiles of 25 wt% CoO/GHCS composite material.

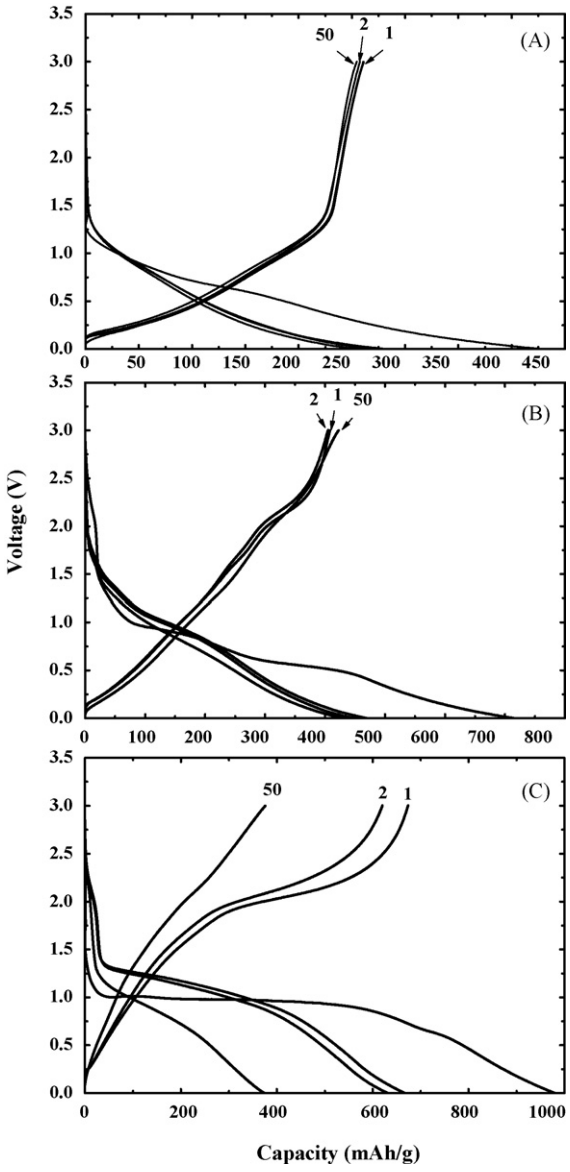

Fig. 5. The comparison of the galvanostatic charge/discharge (100 mA g^{-1}) profiles of the electrodes: (A) the pure GHCS material (B) the 25 wt% CoO/GHCS composite material (C) the 75 wt% CoO/GHCS composite material.

capacity of 258 mAh g^{-1} in the first cycle, corresponding to a coulombic efficiency of 60%. The irreversible capacity of GHCS at the first cycle is mainly attributed to the solid electrolyte interface (SEI) formation and a part of Li-ion inactivation after the first cycle, the degree of which is proportion to the surface area of carbon and the irreversible storage of Li-ions at void or cavity sites that are highly populated in this type of carbon. Although GHCS exhibits a large irreversible capacity during the first cycle, it behaves the stable cyclability, and still remains a discharge capacity of 255 mAh g^{-1} after 50th cycle. The perfect cycle performance could be traced to the combination of a hollow thin-shell geometry and good electrical conductivity from a highly crystalline structure. Compared to other amorphous carbon materials and commercial graphite, GHCS has high graphitable degree to increase electrical conductivity and facilitate the insertion/emersion of Li^+ ions in the solid phase of

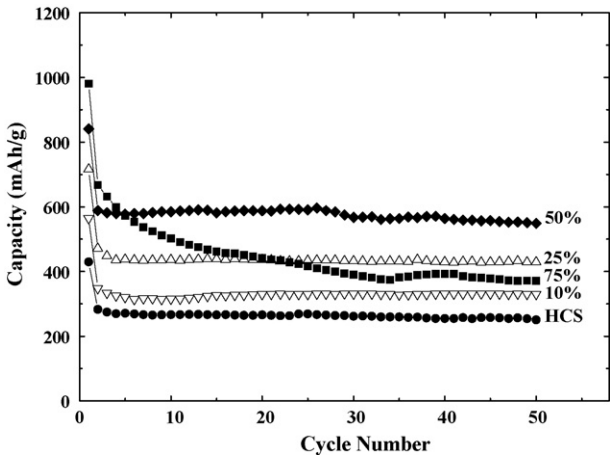

Fig. 6. The comparison of cyclability for CoO/GHCS composites with different CoO content from 0 to 75 wt%.

material; the existence of a hollow structure and porous surface ensures the short diffusion pathways for Li^+ ions transport.

The charge/discharge voltage curve of 25 and 75 wt% CoO/GHCS are shown in Fig. 5B and C, respectively. 25 wt% CoO/GHCS composite delivers a discharge capacity of 716 mAh g^{-1} and charge capacity of 408 mAh g^{-1} in the first cycle, corresponding to a coulombic efficiency of 57% that is close to the coulombic efficiency of GHCS electrode. After 50th cycle, it still remains a discharge capacity of 428 mAh g^{-1}, corresponding to a capacity retention of 91% (vs. 2nd discharge capacity). It is noticed that the discharge curve of 25 wt% CoO-loaded GHCS has not obvious voltage plateau, instead it with a sloping line from 1.0 to 0 V, reflecting the combinative electrochemical behavior of GHCS and CoO particles. The 75 wt% CoO-loaded GHCS has a large initial discharge capacity of 980 mAh g^{-1}, and charge capacity of 700 mAh g^{-1} in the first cycle, but its diacharge capacity reduces rapidly to 371 mAh g^{-1} after 50 cycles with a capacity retention of 56% (vs. 2nd discharge capacity). During the first discharge, the voltage of the cell rapidly drops to 1.0 V with a long plateau which corresponds to the reduction of CoO and the formation of Li_2O, but the voltage plateau rises to about 1.2 V in the subsequent cycles. This is because the CoO particles are pulverized during Li-insertion and their surface energy is decreased due to interaction with the produced Li_2O. In the recharging process, the voltage plateau between 1.5 and 3.0 V becomes less obvious, and the upward slope reflects the regeneration of CoO particles. During the charge/discharge progress, the Li_2O arising from the decomposition of CoO can not be reduced to Li^+ and CoO completely in the subsequent recharging progress, therefore the continuous accumulation of Li_2O per cycle results in the capacity fading.

Fig. 6 compares the cycling stability of CoO/GHSC with different CoO mass loads at a galvanostatic charge/discharge current of 100 mAh g^{-1} between 0 and 3.0 V (vs. Li^+/Li). It is found that the composite materials behave a good cycling stability when the CoO mass load is less than 50 wt%. For example, a capacity retention of 93% after 50 cycle (vs. 2nd discharge capacity) is observed for the CoO/GHCS composite with 50 wt% CoO mass load, while the cycle performance deteriorates rapidly

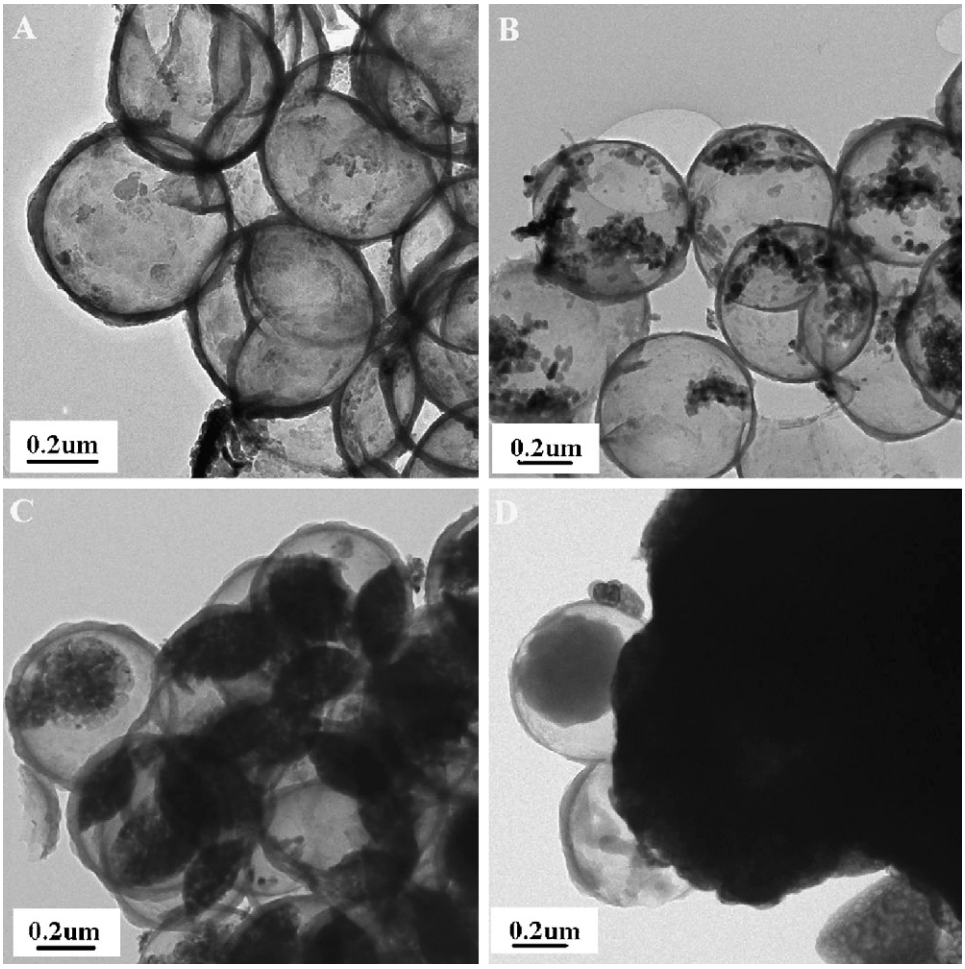

Fig. 7. TEM images of CoO/GHCS composite materials with different CoO contents: (A) 10 wt% (B) 25 wt% (C) 50 wt% and (D) 75 wt%.

when the CoO content reach 75%. It is necessary to answer why CoO/GHCS composite material can obtain different electrochemical performance at the different CoO content? Fig. 7 shows the TEM images of CoO/GHCS composites with different CoO mass loads, varying from 10, 25, 50 to 75 wt%. As shown in Fig. 7A–C, when the CoO mass loads is less than 50 wt%, it is clearly observed that the CoO nanoparticles dispersed well in the inner surface of GHCS. In the model of CoO nanoparticles encapsulated by GHCS, the nano-sized graphite sheet with high surface energy can trap CoO nanoparticles firmly on its inside surface, which prevent CoO from aggregating with other CoO nanoparticles. In addition, the nano-sized CoO closely contacted with graphite sheet ensures a good conductivity and the hollow structure can provide the enough space to buffer the volume change during the Li-ion insertion and extraction reactions in CoO nanoparticles. All of these factors above-mentioned can enhance the cycle ability of CoO/GHCS composite material. Fig. 7D shows the TEM image of 75 wt% CoO/GHCS composite material. From the image, the CoO content is too high so that particles aggregate strongly to form agglomerations. Because the agglomeration of CoO decreases the electrical conductivity between particles, the cycle performance deteriorates rapidly with the 75 wt% CoO content.

Fig. 8 shows the rate performance of 50 wt% CoO/GHCS composite material at different current rates. It delivers a discharge capacity of 535 mAh g^{-1} at 0.3 C (160 mA g^{-1}), 420 mAh g^{-1} at 1.5 C rate, and 282 mAh g^{-1} at the very large rate of 10 C, which remains 53% of the capacity at 0.3 C rate. The measured results demonstrate that the CoO/GHCS composite

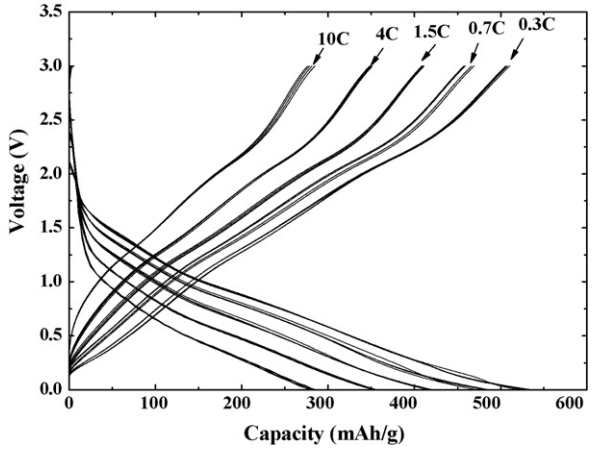

Fig. 8. Rate capabilities of 50 wt% CoO/GHCS composite material.

material behaves a good rate capability. In the reaction of Li-ion insertion/extraction, CoO-loaded hollow carbon spheres have more surface area available for Li-ion diffusion and a shorter lithium-ion diffusion pathway arising from the nanometer-thick carbon shell, and the electron also transfer to the current collector (copper foil) fast throughout close packed carbon spheres. These are desirable attributed for facilitated Li-ion transport that should result in a good rate capacity in applications.

4. Conclusion

In the present work, we prepared the graphitable carbon hollow spheres by silica spheres template and CVD process, and then applied it as dispersing medium to load nano-sized cobalt oxide particles by wet-penetration method. It was found that the core–shell structure CoO/GHCS composite shows the improved cyclability as an anode material in Li-ion battery. The discharge capacity increases with the increase of the CoO mass load, while the cycling stability decreases. Under the optimal condition, the core–shell composite containing 50 wt% CoO exhibits a reversible discharge capacity of 580 mAh g^{-1} at a charge/discharge current of 100 mAh g^{-1} between 0 and 3.0 V (vs. Li^+/Li), and remains a capacity retention of 93% after 50th cycle. The improvement could be attributed to that the graphitable hollow carbon sphere with a good electronic conductivity and high surface severs as depressing medium to prevent CoO from aggregating with other CoO nanoparticles, and provide the enough space to buffer the volume change during the Li-ion insertion and extraction reactions in CoO nanoparticles. The as-synthesized CoO/carbon composite material described in the present work shows high rate capability and excellent cycling ability as an anode for Li-ion batteries. Moreover, it is can be easily extend this synthetic methodology to the preparation of other nano-sized transition-metal oxide for Li-ion battery applications, such as CuO, NiO, Fe_2O_3, etc.

Acknowledgments

This work was partially supported by the National Natural Science Foundation of China (No. 20373014), and the State Key Basic Research Program of PRC (2007CB9700).

References

[1] B. Scrosati, Electrochim. Acta 45 (2000) 2461–2466.
[2] K. Sawai, Y. Iwakoshi, T. Ohzuku, Solid State Ionics 69 (1994) 273.
[3] J.R. Dahn, T. Zheng, Y. Liu, J.S. Xue, Science 270 (1995) 290–293.
[4] P. Poizot, S. Laruelle, S. Grugeon, L. Dupont, J.-M. Tarascon, Nature 407 (2000) 496–499.
[5] J.-S. Do, C.-H. Weng, J. Power Sources 159 (2006) 323–327.
[6] G.X. Wang, Y. Chen, K. Konstantionv, Matthew Lindsay, H.K. Liu, S.X. Dou, J. Power Sources 109 (2002) 142–147.
[7] G.X. Wang, Y. Chen, K. Konstantinov, Jane Yao, Jung-ho Ahn, H.K. Liu, S.X. Dou, J. Alloys Compd. 340 (2002) L5–L10.
[8] R. Yang, Z. Wang, J. Liu, L. Chen, Electrochem. Solid-State Lett. 7 (12) (2004) A496–A499.
[9] H.C. Choi, S.Y. Lee, S.B. Kim, M.G. Kim, M.K. Lee, H.J. Shin, J.S. Lee, J. Phys. Chem. B 106 (2002) 9252–9260.
[10] H. Huang, E.M. Kelder, J. Schoonman, J. Power Sources 114 (2001) 97–98.
[11] J. Hu, H. Li, X.J. Huang, L.Q. Chen, Solid State Ionics 177 (26–32) (2006) 2791–2799.
[12] J. Hu, H. Li, X.J. Huang, Electrochem. Solid-State Lett. 8 (1) (2005) A66–A69.
[13] Y. Wang, F. Su, J. Yang Lee, Chem. Mater. 18 (2006) 1347–1353.
[14] W. Stöber, A. Fink, E. Bohn, J. Colloid Interf. Sci. 26 (1968) 62.